

400 Gbps Dual-polarisation Non-linear Frequency-division Multiplexed Transmission with b-Modulation

Xianhe Yangzhang⁽¹⁾⁽²⁾, Vahid Aref⁽²⁾, Son T. Le⁽²⁾, Henning Bülow⁽²⁾, Polina Bayvel⁽¹⁾

⁽¹⁾ Optical Networks Group, Department of Electronic & Electrical Engineering, UCL, UK
x.yangzhang@ucl.ac.uk

⁽²⁾ Nokia-Bell-Labs, Stuttgart, Germany

Abstract We demonstrate, for the first time, a b-modulated dual-polarisation NFDM transmission in simulation, achieving a record net data rate of 400 Gbps (SE of 7.2 bit/s/Hz) over 960 km. The proposed scheme shows 1 dB Q-factor improvement over q_c -modulation scheme.

Introduction

Nonlinear frequency-division multiplexing (NFDM) has been intensively investigated as a potential transmission scheme to overcome the performance limitation due to the Kerr effect in optical fibre. Under specific conditions, NFDM shows significantly weaker inter-channel interference in comparison to the conventional linear multiplexing schemes, e.g. wavelength-division multiplexing (WDM)^{9,10}. However, despite many respectful endeavours^{1,4}, only up to 2.3 bit/s/Hz⁴ has been achieved in NFDM systems up to date due the two main reasons, namely i) most of NFDM systems up to date use only one polarization for data transmission and ii) severe signal-noise interaction^{1,4}.

To suppress the signal-noise interaction in NFDM transmissions, it is crucial to find the “correct” degrees of freedom offered by non-linear spectrum for data modulation. It has been shown (for single-polarization) that modulating information on the b-coefficient significantly improves the transmission performance compared to the conventional q_c -modulation scheme^{3,8}.

In this work, for the first time, we developed a novel transform which enables b-modulation for dual-polarisation under the constraint $|b_1(\lambda)|^2 + |b_2(\lambda)|^2 < 1$, which outperforms the conventional q_c -modulation² scheme by over 1 dB. In addition, the b-modulated dual-polarisation transmission system is systematically optimised for increasing the data rate. As a result, we achieved in simulation a record net data rate of 400 Gbps with a SE of 7.2 bits/s/Hz over 12 spans of 80 km of standard single mode fibre (SSMF) with EDFAs.

The Optic-fibre Model

The optic-fibre model of concern is a multi-span point-to-point dual-polarisation dispersion unmanaged fibre link with equally-spaced erbium-

Tab. 1: Fibre and system simulation parameters

ν	193.44 THz	centre carrier freq.
α	0.2 dB km ⁻¹	fibre loss
γ	1.3 (W · km) ⁻¹	non-linearity para.
D	16.89 ps/(nm-km)	dispersion para.
W	56 GHz	linear bandwidth
R_o	8	oversampling rate
\mathcal{L}_{sp}	80 km	span length
N_{sp}	12	number of spans
NF	5 dB	EDFA noise figure

doped fibre amplifiers (EDFAs), which can be described by the Manakov equation

$$\frac{\partial \vec{Q}}{\partial z} + \frac{\alpha}{2} \vec{Q} + \frac{j\beta_2}{2} \frac{\partial^2 \vec{Q}}{\partial t^2} - j \frac{8}{9} \gamma \vec{Q} \|\vec{Q}\|^2 = 0$$

where $j = \sqrt{-1}$ and $\vec{Q} = [q_x(t, z) \ q_y(t, z)]$ is the complex envelope of the signal as a function of time t and distance z along the fibre, D , γ , and α are the dispersion, non-linear, and loss coefficients of the fibre; Tab. 1 lists all parameters.

q_c and b-modulation

We explain in this section q_c and b-modulation, respectively. For each NFDM symbol, the standard OFDM is used to construct signal $u_i(\lambda)$

$$u_i(\lambda) = \sum_{k=-N_C/2}^{N_C/2-1} c_i^k \frac{\sin(\lambda T_0 + k\pi)}{\lambda T_0 + k\pi}, \quad i \in \{1, 2\},$$

where k and i is the sub-carrier and polarisation index, c_i^k is chosen from the 32-QAM constellation, $T_0 = N_C/W$, and N_C is the number of sub-carriers. We define $\eta = (T_0 + T_G)/T_0$, where T_G is the guard interval. The discrete signal $\vec{u}_i = [u_i^1, \dots, u_i^n]$ can be implemented by

$$\vec{d}_i = \text{IDFT}\{f(\vec{c}_i, N_C(R_o - 1))\},$$

$$\vec{u}_i = \begin{cases} \text{DFT}\{f(\vec{d}_i, N_C R_o(\eta - 1))\}, & \eta \geq 2, \\ \text{DFT}\{f(\vec{d}_i, N_C R_o)\}, & 1 < \eta < 2, \end{cases}$$

where R_o is the oversampling rate and $f(\vec{x}, N)$ is defined as a function that adds N zeros to vector \vec{x} in the following way

$$f(\vec{x}, N) = \underbrace{[0, \dots, 0]}_{N/2}, x^1, \dots, x^n, \underbrace{[0, \dots, 0]}_{N/2}.$$

For q_c -modulation, the following transform denoted as R in Fig. 2(a) was performed for signals in both polarisations²

$$\begin{aligned} q_{c1}(\lambda) &= \sqrt{e^{|u_1(\lambda)|^2} - 1} \cdot e^{j\angle u_1(\lambda)}, \\ q_{c2}(\lambda) &= \sqrt{e^{|u_2(\lambda)|^2} - 1} \cdot e^{j\angle u_2(\lambda)}. \end{aligned}$$

For b -modulation, the transform R becomes

$$\begin{aligned} A &= \sqrt{\frac{1 - \exp(-|u_1(\lambda)|^2 - |u_2(\lambda)|^2)}{|u_1(\lambda)|^2 + |u_2(\lambda)|^2}}, \\ b_1(\lambda) &= A \cdot u_1(\lambda), \quad b_2(\lambda) = A \cdot u_2(\lambda), \\ a(\lambda) &= \exp(\mathbf{H}(\log(\sqrt{1 - |b_1(\lambda)|^2 - |b_2(\lambda)|^2}))), \end{aligned}$$

where \mathbf{H} stands for the Hilbert transform, explained in⁸. Subsequently, either $\{a(\lambda), b_1(\lambda), b_2(\lambda)\}$ or $\{q_{c1}(\lambda), q_{c2}(\lambda)\}$ will be passed through the inverse NFT to calculate the time domain signal. The transform R for b coefficient facilitates the signal modulation because $u(\lambda)$ ranges the entire complex plane, while $b_1(\lambda)$ and $b_2(\lambda)$ are constraint by $|b_1(\lambda)|^2 + |b_2(\lambda)|^2 < 1$. Note that, for $\eta < 2$, each burst will be truncated symmetrically to a signal of length $N_C R_o \eta$ for transmission and also recovered to length $2N_C R_o$ by adding zeros before NFT processing. At the receiver, the NFT and back rotation equalisation are performed. We demonstrate first the advantage of b -modulation over q_c -modulation in a relatively ideal scenario, i.e., large guard interval. Fig. 1 clearly shows that the non-linear processing penalty (back-to-back) of b -modulation is roughly 1.5 dB in Q-factor smaller than the penalty in q_c -modulation. When signals are transmitted through fibre, extra Q-factor degradation are observed due to the approximation error of path-averaged model in both cases. Note that, in all simulations, pre-compensation⁶ was applied to reduce the temporal broadening caused by dispersion. The power \mathcal{P} reported in this work is always per polarisation.

Optimisation of b -modulated dual-polarisation NFT transmission

Once the advantage of b -modulation is established, we optimise the total data rate over several system parameters providing the optical fibre

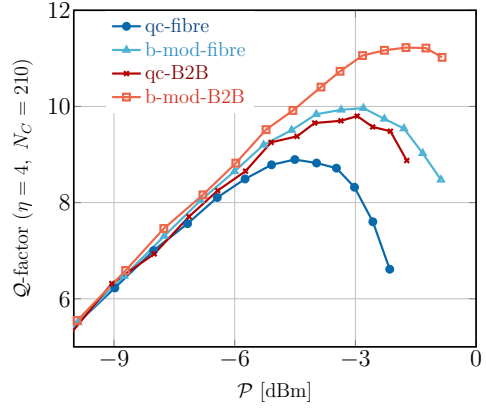


Fig. 1: Comparison of q_c and b modulation with large guard interval $\eta = 4$ in both back-to-back case and fibre transmission. The total additive noise powers are the same.

channel specified by Tab. 1. The available optimisation parameters are number of sub-carriers N_C , the ratio η and launch power per polarisation \mathcal{P} . The optimisation process can be simplified by estimating the required guard interval⁴

$$T_G \approx \pi W \beta_2 L = 3.75 \text{ ns}.$$

T_G depends only on signal bandwidth and transmission distance and thus, should remain constant in this work. As defined earlier,

$$\eta = (T_0 + T_G)/T_0 = 1 + WT_G/N_C.$$

For instance, if $\eta = 2$, $N_C = 210$. Any further reduction of η should be achieved by increasing N_C , consequently the spectral efficiency (SE) loss due to guard interval will diminish. However, for large N_C , non-linear processing (NFT or INFT) penalty will become more severe, resulting in a Q-factor degradation. The non-linear processing penalty is attributed to two factors: 1) inaccuracy of algorithms for high-energy pulses, 2) energy-dependent signal-noise interaction.

Fig. 3 shows the further optimisation results with smaller η . It can be seen from Fig. 3(a) that reducing η will increase the non-linear processing penalty. In terms of spectral efficiency MI/η , the benefit of reducing η is more significant than the information loss due to the increased non-linear processing penalty, until the threshold $\eta = 1.2$ as shown in Fig. 3(b). Furthermore, we quantify the noise induced by algorithmic inaccuracy with simulations in the absence of additive noise. Fig. 2(b) shows that the algorithmic inaccuracy becomes the primary limitation on the achievable mutual information rate at high power providing the same R_o and η and worsens with increasing N_C . The finding is also in consistency with

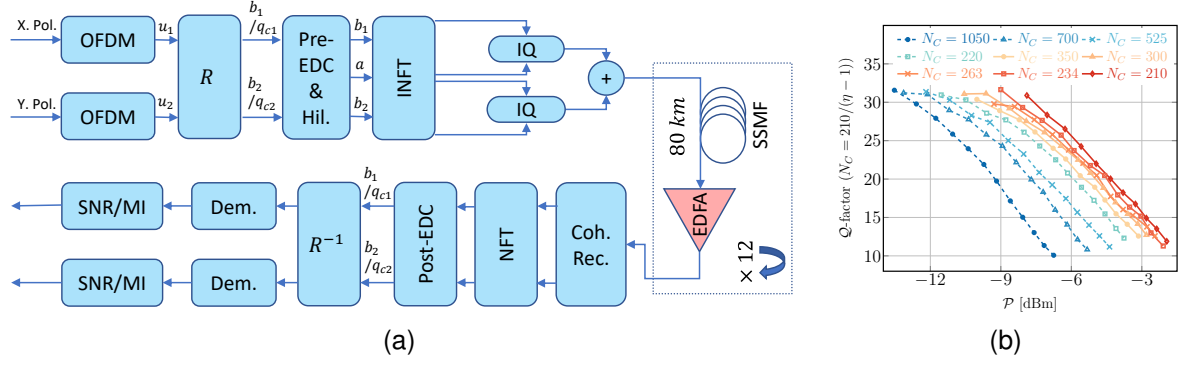


Fig. 2: Simulation diagram (a) and its noiseless back-to-back characterisation (b).

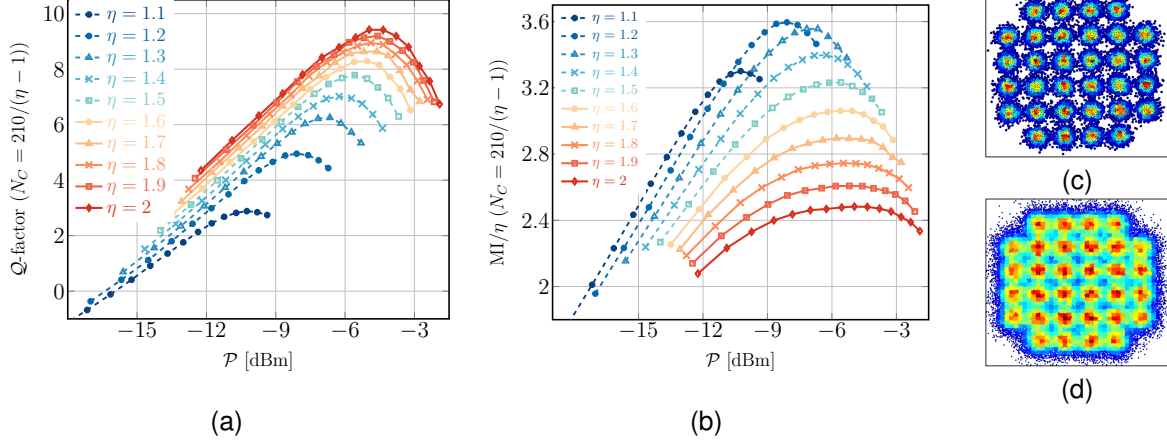


Fig. 3: Further decrease of η and its impact on Q-factor and MI/η (SE). (c) is the received constellation at the point of maximum Q-factor in (a). (d) is the received constellation at the point of maximum MI/η in (b).

the results in⁵⁷. The required spectral resolution increases as $|b_1(\lambda)|^2 + |b_2(\lambda)|^2$ approaches 1. Finally, by choosing $\eta = 1.2$, at power of -8 dBm per polarisation, we achieved a spectral efficiency of 3.6 bits/s/Hz per polarisation, resulting 400 Gbps net data rate, while the gross data rate is 560 Gbps. Should the algorithmic accuracy be improved, higher data rate or SE is expected.

Conclusions

In conclusion, our contribution in this work is threefold: 1) we developed a transform that enables polarisation-multiplexed b -modulation under the constraint $|b_1(\lambda)|^2 + |b_2(\lambda)|^2 < 1$, 2) we demonstrated that, when using the continuous nonlinear spectrum, modulating b coefficient instead of q_c can provide a significant performance improvement in polarisation-multiplexed NFDM system, 3) We optimised the system for higher data rate and achieved a record high net data rate of 400 Gbps with a SE of 7.2 bits/s/Hz. Higher data rate can be expected once we improve the algorithmic accuracy.

Acknowledgements

The work is within the COIN project, financed by the European Commission grant 676448, under the call H2020-MSCA-ITN-2015.

References

- [1] V. Aref et al. Modulation over nonlinear fourier spectrum: Continuous and discrete spectrum. *J. Lightw. Technol.*, 36(6):1289–1295, Mar 2018.
- [2] J.-W. Goossens et al. Polarization-division multiplexing based on the nonlinear fourier transform. *Opt. Express*, 25(22):26437–26452, Oct 2017.
- [3] S. T. Le et al. 100 gbps b-modulated nonlinear frequency division multiplexed transmission. In *OFC*, pages 1–3, San Diego, US, Mar 2018.
- [4] S. T. Le et al. High speed precompensated nonlinear frequency-division multiplexed transmissions. *J. Lightw. Technol.*, 36(6):1296–1303, Mar 2018.
- [5] I. T. Lima et al. Computational complexity of nonlinear transforms applied to optical communications systems with normal dispersion fibers. In *IPC*, pages 277–278, Reston, VA, USA, Oct 2015.
- [6] I. Tavakkolnia et al. Dispersion pre-compensation for nft-based optical fiber communication systems. In *CLEO, SM4F.4*, Jun 2016.
- [7] V. Vaibhav. Fast inverse nonlinear fourier transform. [arXiv:1706.04069](https://arxiv.org/abs/1706.04069), Dec 2017.
- [8] S. Wahls. Generation of time-limited signals in the nonlinear fourier domain via b-modulation. In *ECOC, W.3.C.6*, Sep 2017.
- [9] X. Yangzhang et al. Impact of perturbations on nonlinear frequency-division multiplexing. *J. Lightw. Technol.*, 36(2):485–494, Jan 2018.
- [10] M. I. Yousefi et al. Linear and nonlinear frequency-division multiplexing. In *ECOC, Düsseldorf, Germany*, Sep 2016.